Soft X-ray Emission and Lithium Production in Cen X-4 during Quiescence

Shin-ichiro Fujimoto,[1] Ryuichi Matsuba,[2] and Kenzo Arai[3]

[1] Department of Electronic Control, Kumamoto National College of Technology,
2659-2 Suya, Koshi, Kumamoto 861-1102, Japan
[2] Institute for e-Learning Development, Kumamoto University, Kumamoto 860-8555, Japan
[3] Department of Physics, Kumamoto University, Kumamoto 860-8555, Japan
E-mail(SF): fujimoto@ec.knct.ac.jp

ABSTRACT

We investigate emission mechanism of soft X-ray radiation from a neutron star soft X-ray transient (NSSXT), Cen X-4 and unusually high abundances of Li on a low-mass secondary in Cen X-4 during a quiescent state. An accretion flow in NSSXTs in quiescence is though to be an advection-dominated one and truncated by magneto-centrifugal forces due to the magnetic field of a neutron star. The advection dominated accretion flow (ADAF) is very hot ($> 1\,\mathrm{MeV}$) enough to synthesize abundant neutrons through the spallation of ^{4}He via protons in the flow. Although almost all charged nuclei in the ADAF are outflowed by the magneto-centrifugal forces, the neutrons accrete onto the neutron star because of no influence of the magnetic field on the neutrons. Consequently, the accretion flow is composed of neutrons near the neutron star. The accretion energy of the neutrons liberated on the surface of the star is a possible energy budget for soft X-ray radiation in a NSSXT in quiescence. Moreover, Li is abundantly synthesized in the ADAF through $\alpha - \alpha$ reactions and is transfered to the surface of the secondary by the magneto-centrifugal forces. We find that for reasonable values of the mass accretion rate and the magnetic field of the neutron star, the estimated soft X-ray luminosity and abundance of Li on the secondary are comparable to those observed in Cen X-4.

KEY WORDS: Accretion, accretion disks — neutron stars — nuclear reactions, nucleosynthesis, abundances — stars: abundances

1. Introduction

X-ray emission from neutron star soft X-ray transients (NSSXTs) in quiescence is phenomenologically fitted with two components, a blackbody-like soft component and power-law hard component. Although the origin of the hard component is still unclear, there are two scenarios for the soft X-ray component. The energy source for the blackbody-like, soft X-ray is interpreted as deep crustal heating (Brown et al., 1998; Rutledge et al., 2001a,b). However, the quiescent state of Cen X-4 is variable on timescales (at a factor of ~ 0.4, ~ 3, and ~ 0.45 in 5 yr (Rutledge et al., 2001a), a few days (Campana et al., 1997), and down to $\sim 100\,\mathrm{s}$ (Campana et al., 2004), respectively). This could rule out the scenario of the energy source due to the deep crustal heating.

The other energy budget for the soft X-ray radiation is residual polar accretion onto a neutron star from a quasi spherical advection dominated accretion flow (ADAF) (Zhang et al., 1998; Menou et al., 1999), which possibly exists around the neutron star during quiescence (Narayan et al., 1996, 1997). Due to magnetic

fields and fast rotation of the neutron star, accreting material is expelled through propeller effects, which cause winds driven via magneto-centrifugal forces when a mass accretion rate is sufficiently low. Even when the propeller effects operate, accretion through the polar region of the star is possible because of weak centrifugal forces in the region. The fraction of the mass accretion rate that reached the neutron star surface has been estimated to be $\sim 10^{-3}$ for reasonable values of the mass accretion rate and magnetic field of the star (Menou et al., 1999). However, the fraction could be much lower if the accretion flow has a toroidal morphology with empty funnels along the rotational axis (Menou et al., 1999). We note that the MHD simulation of an ADAF show that the flow has funnels with densities lower than that at the equatorial plane (Machida et al., 2004).

ADAF has very low density, so that ions interact inefficiently with electrons. As a result of the inefficient interaction between the ions and the electrons, which are main coolant in ADAF, the ions have high temperatures due to viscous heating and attain to $\sim 30\,\mathrm{MeV}$ near an

inner edge of ADAF (Narayan & Yi, 1994, 1995a,b). Due to such high temperatures, helium breaks via the spallation with protons to produce neutrons in ADAF. Due to magneto-centrifugal forces, almost all charged particles are ejected from an inner region of the ADAF. However, neutrons continues to accrete onto the neutron star, since neutrons are not affected by the magnetic field of the neutron star. As the neutrons liberate almost all its gravitational binding energy onto the surface of the neutron star, the liberated energy is a possible energy budget for the blackbody-like, soft X-ray radiation.

Moreover, Li produced in ADAFs by α-α reactions transports to a secondary star through the propeller effects (Yi & Narayan, 1997). The transportation enhances the Li abundance on the low-mass secondary, and causes a high abundance of Li observed on the low-mass secondary in a NSSXT, Cen X-4 (Martin et al., 1994). We note that Li is destroyed in the deep convective envelope of usual late-type stars, and that high abundances of Li have been detected in late-type secondaries of black hole soft X-ray transients (BHSXTs) in quiescence (Wallerstein, 1992; Martin et al., 1992, 1994, 1996), and have been examined by Fujimoto et al. (2008) (hereafter FMA08). As we can see later, the estimated soft X-ray luminosity and abundance of Li on the secondary are comparable to those observed in Cen X-4, for reasonable values of the mass accretion rate and magnetic field of the neutron star.

In the present study, we propose a new mechanism to produce a soft X-ray radiation from NSSXTs, that is the liberation of the gravitational energy of neutrons on the surface of the star accreting through a neutron-ADAF. We also examine production of Li through the transportation of Li from the ADAF to the secondary.

The paper is organized as follows: in §2, we examine an abundance distribution in an accretion flow around a neutron star. We estimate the soft X-ray luminosity, which is interpreted as the energy liberation of neutrons accreted through a neutron accretion flow in §3. In §4, we examine Li production on a secondary in NSSXTs. Finally we summarize our results in §5.

2. Abundance distribution in an advection dominated accretion flow

We assume that an accretion flow around a neutron star is an ADAF in quiescence in the present study. The temperature of ions in ADAFs is comparable to virial temperature, and is given at radius r by (Narayan & Yi, 1994, 1995a,b);

$$T = 3.7 \times 10^{12} \frac{r_{\rm in}}{r} \, {\rm K} = 31.9 \frac{r_{\rm in}}{r} \, {\rm MeV}. \qquad (1)$$

Here $r_{\rm in}$ is the radius at the inner edge of the ADAF, and is set to be $3r_g$, where r_g is the Schwarzschild radius

for a neutron star with mass $M = 1.4 M_\odot$. We note that $r_{\rm in}$ becomes much greater during the operation of the propeller effects, which will be discussed later. The number density is given by

$$n = 1.7 \times 10^{18} \alpha^{-1} m^{-1} \dot{m} \left(\frac{r}{r_{\rm in}} \right)^{-3/2} {\rm cm}^{-3}, \qquad (2)$$

where α is the viscous parameter, $m = M/M_\odot$, and $\dot{m}$ is the mass accretion rate in units of the Eddington accretion rate $\dot{M}_{\rm Edd} = 1.4 \times 10^{17} m \, {\rm g \, s}^{-1} = 2.1 \times 10^{-9} m \, M_\odot \, {\rm yr}^{-1}$.

Once the temperatures, densities and drift timescales are specified, we can follow the abundance evolution in an ADAF from the outer boundary $r_{\rm out}$ to $r_{\rm in}$, using a nuclear reaction network. We set $r_{\rm out}$ to be $100 \, r_g$. It is likely that $r_{\rm out}$ becomes much larger during the quiescent state (Narayan et al., 1997), but the abundance distribution in the ADAF is independent from the choice of larger $r_{\rm out}$ because of low temperatures ($< 1 \, {\rm MeV}$) in the outer region (Guessoum & Kazanas, 1999). We have developed a nuclear reaction network, in which four $\alpha - \alpha$ reactions to synthesize ^{6}He,^{6}Li,^{7}Li, and ^{7}Be are taken into account, based on a network in FMA08. Our network contains 21 species of nuclei; n, p, D, T, ^{3}He, ^{4}He, ^{6}He, ^{6}Li, ^{7}Li, ^{7}Be, ^{9}B, ^{11}C, ^{12}C, ^{13}N, ^{14}N, ^{15}O, ^{16}O, ^{17}F, ^{20}Ne, ^{21}Na, and ^{24}Mg, and 18 reactions, whose rates are taken from Table 1 in (Guessoum & Gould, 1989) or thermally averaged with experimental cross sections (Read & Viola, 1984) for $\alpha - \alpha$ reactions. It should be emphasized that photodisintegration reactions are not important for abundance evolution inside ADAFs, since the ADAF is optically thin and photons have no chance to interact with nuclei due to low gas densities (Eq. (2)). Initial abundance at $r_{\rm out}$ is set to be the solar composition (Anders & Grevesse, 1989) without Li.

Figure 1 shows the abundance distribution of neutrons, ^{4}He, ^{6}Li, ^{7}Li, and ^{7}Be inside ADAFs for $\alpha = 0.3$, $m = 1.4$, and $\dot{m} = 0.01$ and 0.1. Neutrons are produced significantly via the breakup of ^{4}He at an inner region ($r < 20 r_g$). The distribution of neutrons is similar to that in Figure 1 of (Jean & Guessoum, 2001). Lithium is appreciably synthesized at the inner region of the ADAF. ^{7}Be is comparable to and slightly lower than ^{7}Li, while ^{6}He is much lower than ^{6}Li. We note that the number fraction of neutrons $Y_{\rm n}$ and Li abundances depends not on m solely, but on the combination $\dot{m}/\alpha^2$. Hereafter we fix $\alpha = 0.3$ in the present paper (Narayan et al., 1997).

3. New interpretation of soft X-ray emission in terms of neutron-ADAF

The very low mass accretion rates on to a neutron star ($\leq 10^{-5}$ in units of $\dot{M}_{\rm Edd}$ (Asai et al., 1996)) have been suggested the termination of mass accretion via the propeller effects, which can explain a sudden spectral
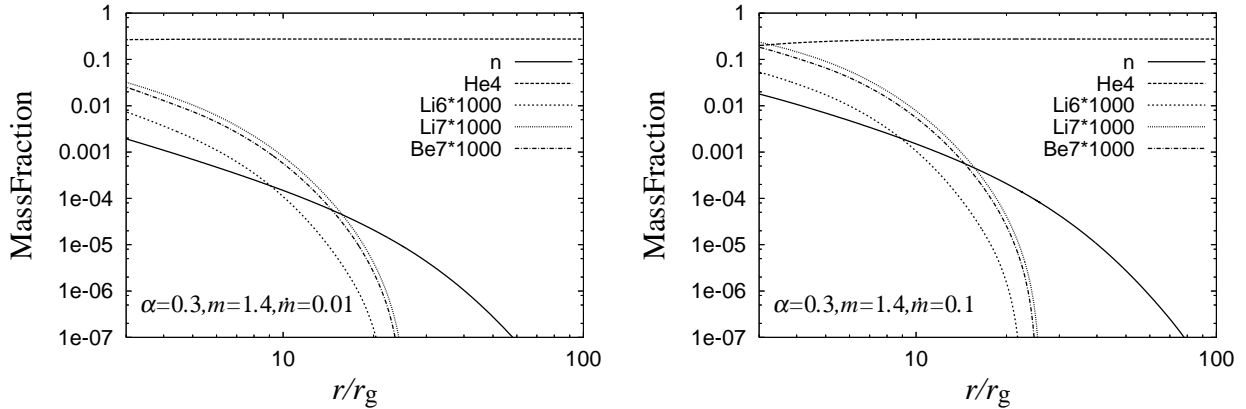
Fig. 1. Abundance distribution in ADAFs for $\alpha = 0.3$, $m = 1.4$, and $\dot{m} = 0.01$ (left panel) and 0.1 (right panel). The solid, dashed, short-dashed, dotted, and dash-dotted lines indicate the mass fractions of n, ^{4}He, ^{6}Li, ^{7}Li, and ^{7}Be, respectively.

state transition observed in X-ray from three NSSXTs, Aql X-1 (Campana et al., 1998; Zhang et al., 1998), SAX J1808.4-3658 (Gilfanov et al., 1998), and 4U 1608-52 (Chen et al., 2006). Through the propeller effects, the material is ejected from ADAF around the ejection radius $r_{\rm ej}$, which is given by the Alfvén radius,

$$r_{\rm ej} = 9.74 \left(\frac{B_{\rm NS}}{10^8 \rm G} \right)^{4/7} \left(\frac{m}{1.4} \right)^{-2/7} \left(\frac{\dot{m}}{0.01} \right)^{-2/7} r_g, (3)$$

if $r_{\rm ej}$ is larger than the corotation radius (Yi & Narayan, 1997),

$$r_c = 9.4 \left(\frac{m}{1.4} \right)^{1/3} \left(\frac{P_{\rm NS}}{1 \, \rm msec} \right)^{2/3} \rm km, \qquad (4)$$

otherwise the propeller effects do not work. Here, $B_{\rm NS}$ and $P_{\rm NS}$ are the magnetic field and the rotational period of the neutron star, respectively. Figure 2 shows $r_{\rm ej}$ for $B_{\rm NS} = 10^8 \rm G$ (dashed line) and $10^9 \rm G$ (dotted line) as a function of $\dot{m}$. We also show the radius where the mass fraction of ^{7}Li equals to 10^{-7} in the ADAF (solid line).

The propeller effects operating in NSSXTs during quiescence have important meaning to an accretion flow around the neutron star. As shown in Figure 1, appreciable fractions of neutrons are produced in the ADAF at $r_{\rm ej}$, which is smaller than 20 r_g for a reasonable set of parameters (Figure 2). Although almost all charged particles are ejected due to magneto-centrifugal forces near $r_{\rm ej}$, neutrons are not affected by the magnetic field of the neutron star because of the charge-less of neutrons. Consequently, even after the operation of the propeller effects, accretion of neutrons continues to take place onto the neutron star, and a *neutron-ADAF* is formed around the neutron star.

As the neutron-ADAF emits little radiation during accretion, the neutrons accreting onto the neutron star liberate almost all its gravitational binding energy onto the
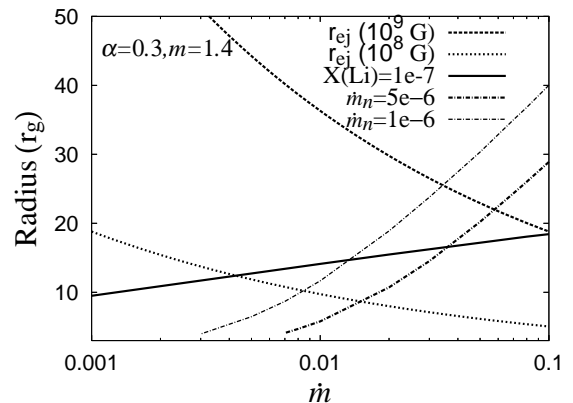

Fig. 2. Radius where the mass fraction of ^{7}Li equals to 10^{-7} in the ADAF, $r(\rm Li)$, and ejection (Alfvén) radius $r_{\rm ej}$ vs mass accretion rates. Solid, dashed, and dotted lines indicate $r(\rm Li)$, $r_{\rm ej}$ for the magnetic field of the neutron star $B_{\rm NS} = 10^8 \rm G$, and $r_{\rm ej}$ for $B_{\rm NS} = 10^9 \rm G$, respectively, in units of r_g. We also present radii where a mass accretion rate of neutrons $\dot{m}_n$ equals to 1×10^{-6} (thin dash-dotted line) or 5×10^{-6} (dash-dotted line).

surface of the neutron star. The liberated energy is a possible candidate for a energy budget of the blackbody-like, soft X-ray radiation. If we interpret the soft X-ray radiation of $\sim 10^{32} \, \rm erg \, s^{-1}$ as the energy liberation onto the neutron star through the neutron-ADAF, a mass accretion rate of neutrons through the neutron-ADAF $\dot{m}_n \sim 10^{-6}$ is required in units of the Eddington accretion rate. We note that the quiescent soft X-ray luminosity in Cen X-4 is $2 - 3 \times 10^{32} \, \rm erg \, s^{-1}$ (Asai et al., 1998).

We have evaluated $\dot{m}_n = \dot{m} X_{\rm n, ADAF}$, assuming $r_{\rm ej} > r_c$, where $X_{\rm n, ADAF}$ is the mass fraction of neutrons at $r_{\rm ej}$. For a given $\dot{m}$, higher $B_{\rm NS}$ means larger $r_{\rm ej}$ and thus smaller $\dot{m}_n$ because of smaller $X_{\rm n, ADAF}$. The blackbody-

like, soft X-ray emission with an order of $10^{32} \, \mathrm{erg\,s^{-1}}$ requires $\dot{m} \geq 7 \times 10^{-3}$ for a neutron star with $B_{\mathrm{NS}} \geq 10^{8} \, \mathrm{G}$. Radii where $\dot{m}_n$ equals to 1×10^{-6} (thin dash-dotted line) or 5×10^{-6} (dash-dotted line) are shown in Figure 2.

4. Transportation of Li to the secondary through the propeller effect

The material in an ADAF is outflowed via the propeller effects, so that a fraction of Li produced in the ADAF can be transfered to the secondary and enhance Li abundances on the secondary. A fraction of the Li on the secondary is returned to the ADAF through mass accretion. We can estimate an equilibrium abundances of Li. For isotropic ejection of Li from the ADAF, the production rate of Li on the secondary is given by

$$\dot{M}_{\mathrm{Li}}^{+} = \dot{M} X_{\mathrm{Li,ADAF}} \left(\frac{R_*}{a} \right)^2, \qquad (5)$$

where $X_{\mathrm{Li,ADAF}}$, R_* and a are the mass fraction of Li (^{6}Li and ^{7}Li) at an ejection radius of the ADAF, r_{ej}, the radius of the secondary, and the binary separation, respectively. While the mass transfer rate of Li from the surface to the ADAF is expressed as $\dot{M}_{\mathrm{Li}}^{-} = \dot{M} X_{\mathrm{Li}}$, where X_{Li} is the mass fraction of Li on the secondary. For equilibrium between the production and loss rates $\dot{M}_{\mathrm{Li}}^{+} = \dot{M}_{\mathrm{Li}}^{-}$, one can obtain an equilibrium Li abundance

$$Y_{\mathrm{Li,\,eq}} = \frac{1}{7} \left(\frac{R_*}{a} \right)^2 X_{\mathrm{Li,ADAF}}, \qquad (6)$$

where an averaged mass number of Li, $\bar{A}_{\mathrm{Li}}$, is set to be 7, because of larger fractions of ^{7}Li compared with ^{6}Li, as shown in Figure 1.

We find that $Y_{\mathrm{Li,\,eq}}$ is comparable to the observed Li abundances in Cen X-4 ($6.67 \times 10^{-10}(Y_p/0.9)$ (Casares et al., 2007)) for $X_{\mathrm{Li,ADAF}} = 0.817 \times 10^{-7}$, which is realized at $\sim 14r_g$ and $\sim 18r_g$ in the ADAF for $\dot{m} = 0.01$ and 0.1, respectively (Figure 1). We note that Li isotopic ratios ^{6}Li/^{7}Li in the ADAF at the above radii are 0.19, which is comparable to the observed ratio in Cen X-4 ($0.12^{+0.08}_{-0.05}$) (Casares et al., 2007). Moreover, we find that for $\dot{m} \sim 0.01-0.02$ and $B_{\mathrm{NS}} = 2-3 \times 10^8 \, \mathrm{G}$, the estimated values for the Li abundance as well as the soft X-ray luminosity are comparable to the observed values.

We note that the estimate for Li abundance is largely different from that in (Yi & Narayan, 1997), because they have only considered the decrease in Li due to nuclear burning and have ignored the decrease in Li via mass accretion, which is much larger than that through Li burning, in a short time scale of years. It should be emphasized that $Y_{\mathrm{Li,\,eq}}$ depends on α and $\dot{m}$ as the combination of $\dot{m}/\alpha^2$, as well as r_{ej}, through $X_{\mathrm{Li,ADAF}}$.

It should be emphasized that the accretion rates, $\dot{m} \sim 0.01 - 0.02$, are comparable to $1/3$ of the mass transfer rate predicted by binary evolution models (King et al., 1996; Menou et al., 1999) for a secondary mass of $0.23 M_\odot$ and the orbital period of 0.629 day (Casares et al., 2007) and is consistent with an averaged rate estimated by Heinke et al. (2007) based on an outburst luminosity and a quiescent duration. We note that the magnetic field of the neutron star has been estimated as $\sim 2 \times 10^9 \, \mathrm{G}$ by Zhang et al. (1998), although in their evaluation they adopted a state change luminosity and a spin period of the star, which are uncertain.

5. Summary

We have proposed the emission mechanism of soft X-ray radiation from NSSXTs and have examined unusually high abundances of Li on a low-mass secondary in Cen X-4 during a quiescent state. Inside the hot ($> 1 \, \mathrm{MeV}$) ADAF around a neutron star, neutrons are abundantly synthesized through the spallation of ^{4}He via protons in the flow. We find that the neutron-ADAF is formed around the neutron star after the operation of the propeller effects. The accretion energy of the neutrons liberated on the surface of the star is a possible energy budget for soft X-ray radiation in a NSSXT in quiescence. Moreover, Li is abundantly synthesized in the ADAF through $\alpha - \alpha$ reactions and is transfered to the surface of the secondary by the magneto-centrifugal forces. We find that the estimated soft X-ray luminosity and abundance of Li on the secondary are comparable to observed values in Cen X-4 for reasonable values of the mass accretion rate and the magnetic field of the neutron star, or $2 - 4 \times 10^{-11} M_\odot \, \mathrm{yr}^{-1}$ and $1 - 2 \times 10^8 \, \mathrm{G}$, respectively. We also find that the isotopic ratio of lithium ^{6}Li/^{7}Li is found to be comparable to an observed ratio in Cen X-4.

References

Anders, E., & Grevesse, N. 1989, Geochim. Cosmochim. Acta 53, 197

Asai, K., et al. 1996, PASJ, 48, 257

Asai, K., Dotani, T., Hoshi, R., Tanaka, Y., Robinson, C. R., & Terada, K. 1998, PASJ, 50, 611

Brown, E. F., Bildsten, L., & Rutledge, R. E. 1998, ApJ, 504, 95

Campana, S., Mereghetti, S., Stella, L., & Colpi, M. 1997, A&A, 324, 941

Campana, S., et al. 1998, ApJ, 499, L65

Campana, S., Israel, G. L., Stella, L., Gastaldello, F., & Mereghetti, S. 2004, ApJ, 601, 474

Casares, J., Bonifacio, P., González Hernández, J. I., Molaro, P., & Zoccali, M. 2007, A&A, 470, 1033

Chen, X., Zhang, S. N., & Ding, G. Q. 2006, ApJ, 650, 299

Fujimoto, S., Matsuba, R., & Arai, K. 2008, ApJ, 673, 51 (FMA08)

Garcia, M. R., McClintock, J. E., Narayan, R., Callanan, P., Barret, D., & Murray, S. S. 2001, ApJ, 553, L47

Gilfanov, M., Revnivtsev, M., Sunyaev, R., & Churazov, E. 1998, A&A, 338, L83

Guessoum, N., & Gould, R. J. 1989, ApJ, 345, 356

Guessoum, N., & Kazanas, D. 1999, ApJ, 512, 332

Heinke, C. O., Jonker, P. G., Wijnands, R., & Taam, R. E. 2007, ApJ, 660, 1424

Jean, P., & Guessoum, N. 2001, A&A, 378, 509

King, A. R., Kolb, U., & Burderi, L. 1996, ApJ, 464, L127

Machida, M., Nakamura, K., & Matsumoto, R. 2004, PASJ, 56, 671

Martin, E. L., Rebolo, R., Casares, J., & Charles, P. A. 1992, Nature, 358, 129

Martin, E. L., Rebolo, R., Casares, J., & Charles, P. A. 1994, ApJ, 435, 791

Martin, E. L., Casares, J., Charles, P. A., & Rebolo, R. 1995, A&A, 303, 785

Martin, E. L., Casares, J., Molaro, P., Rebolo, R., & Charles, P. 1996, New Astron. 1, 197

Menou, K., Esin, A. A., Narayan, R., Garcia, M. R., Lasota, J.-P., & McClintock, J. E. 1999, ApJ, 520, 276

Narayan, R., & Yi, I. 1994, ApJ, 428, L13

Narayan, R., & Yi, I. 1995a, ApJ, 444, 231

Narayan, R., & Yi, I. 1995b, ApJ, 452, 710

Narayan, R., McClintock, J. E., & Yi, I. 1996, ApJ, 457, 821

Narayan, R., Barret, D., & McClintock, J. E. 1997, ApJ, 482, 448

Read, S. M., & Viola, V. E., Jr. 1984, Atomic Data and Nuclear Data Tables, 31, 359

Rutledge, R. E., Bildsten, L., Brown, E. F., Pavlov, G. G., & Zavlin, V. E. 2001, ApJ, 551, 921

Rutledge, R. E., Bildsten, L., Brown, E. F., Pavlov, G. G., & Zavlin, V. E. 2001, ApJ, 559, 1054

Wallerstein, G. 1992, Nature, 356, 569

Yi, I., & Narayan, R. 1997, ApJ, 486, 363

Zhang, S. N., Yu, W., & Zhang, W. 1998, ApJ, 494, L71